Comparison of mass transfer coefficient approach and Nernst–Planck formulation in the reactive transport modeling of Co, Ni, and Ag removal by mixed-bed ion-exchange resins

Martin Bachet, Loïc Jauberty, Laurent De Windt, Etienne Tevissen, Caroline De Dieuleveult, Hélène Schneider

The comparison of mass transfer coefficient approach and Nernst-Planck formulation in the reactive transport modeling of Co, Ni and Ag removal by mixed-bed ion-exchange resins

Martin Bachet[1,2*], Loïc Jauberty[2], Laurent De Windt[2], Etienne Tevissen[3], Caroline de Dieuleveult[2], Hélène Schneider[1]

(1) Dpt. Matériaux et Mécanique des Composants, EDF R&D, 77818 Moret sur Loing cedex (France).

(2) Centre de Géosciences, Mines-ParisTech, 77305 Fontainebleau cedex (France).

(3) DEN/CAD/STCP/LHC, CEA, 13108 Saint-Paul lez Durance cedex (France).

(*) Corresponding author: Dpt. Matériaux et Mécanique des Composants, EDF, Avenue des Renardières - Ecuelles 77818 Moret sur Loing cedex (France); tel: +33-1-60.73.63.44; fax: +33-1-60.73.68.89; email: martin.bachet@edf.fr

Abstract

Experiments performed under chemical and flow conditions representative of pressurized water reactors (PWR) primary fluid purification by ion exchange resins (Amberlite IRN9882) are modeled with the OPTIPUR code, considering 1D reactive transport in the mixed-bed column with convective/dispersive transport between beads and electro-diffusive transport within the boundary film around the beads. The effectiveness of the purification in these dilute conditions is highly related to film mass transfer restrictions, which are accounted for by adjustment of a common mass transfer coefficient (MTC) on the experimental initial leakage or modeling of species diffusion through the bead film by the Nernst-Planck equation. A detailed analysis of the modeling against experimental data shows that the Nernst-Planck approach with no adjustable parameters performs as well as, or better, than the MTC approach, particularly to simulate the chromatographic elution of silver by nickel and the subsequent enrichment of the solution in the former metal.

Keywords: ion exchange resin, mass transfer coefficient, Nernst-Planck, nickel, reactive transport, ultrapure water.

Introduction

All nuclear power plants require water treatment to remove corrosion products from the primary circuit. For instance, pressurized water reactors (PWR) change from reducing conditions in the primary coolant to oxidizing conditions during shutdown. This transient is associated with an important release of activated corrosion products (among others cobalt, nickel and silver), which have to be removed from the coolant by mixed-bed ion exchange resins. Mixed bed consists of a mixture of cation- and anion-exchange resins, resulting in simultaneous removal of cation and anion from the bulk solution. The resin purification contributes to radiation protection (dose rates due to radionuclides such as ^{110m}Ag, ^{58}Co and ^{60}Co), to control feed system fouling, and to keep materials performance. Mixed-bed ion exchange is also extensively used to yield ultrapure water in microelectronics and pharmaceutical industries. In order to improve removal efficiency of the resin processes and to limit the amount of waste, mechanism of purification by resins has to be better understood and their lifespan predicted. With this respect, the reactive transport modeling of an operating resin is a useful tool coupling the hydrodynamics to the chemical reactions (multi-ionic exchanges but also aqueous acid/base reactions and complexation).

The conditions of low solute concentrations and high flow rates complicate the numerical implementation of such modeling approaches. Moreover, the requirement of ultra high purification means that the resin has to be changed well before its full saturation state. The modeling of the decontamination factor, which is a key issue in this study, needs for a fine simulation at the interface liquid/bead to simulate as accurately as possible the early leakage of metallic contaminants. As demonstrated in the literature[1–3], the rate limiting step in ion exchange with ultrapure water is the film diffusion between the bulk of the column and the resin beads. Only a very few models able to tackle with both the kinetics of hydrodynamic as well as a multicomponent chemistry have been published so far[3–5].

This study deals with the modeling of a series of experiments designed for chemical and flow conditions representative of the purification process of a French PWR primary circuit, conditions that can be generalized to other types of reactors. The OPTIPUR code[6] is applied to simulate the 1D reactive transport in the mixed-bed column with convective/dispersive transport between the beads and electro-diffusive transport within the boundary layer around the beads. Two methods of progressive complexity are compared to model the film diffusion limitation: a single mass-transfer coefficient for all dissolved species and a Nernst-Planck formulation that considers the specific diffusion of each charged species as well as their electrical interactions within the Nernst film. A main novelty of the present study is to make a detailed comparison and analysis of the modeling approach against the experimental data.

Experimental set-up

Water chemistry

The fluid of the primary system in French pressurized water reactors is an aqueous solution consisting mainly of a mixture of boric acid ($B(OH)_3$) and lithium hydroxide (LiOH), in varying proportions depending on the operational stage. Table 1 provides information on the chemistry of the synthetic primary fluid considered in this study, which is within the range typically observed during reactor shutdown, except for the sulfate ions that would typically be at ultra-trace levels in a primary circuit. The concentrations of boron and lithium used in the column tests were about 2750 mg/L and 1 mg/L, respectively. The pH was in the range 5 – 5.5 at 25 °C. All tests were carried out on initially pure resins in the form H^+ and OH^- for the cationic and anionic components, respectively.

The injection solution was produced by online mixing of the primary solution with a concentrated solution of $NiSO_4$, $CoSO_4$ and Ag_2SO_4 salts, the nickel concentration being about 50 times higher than the cobalt and silver ones. The injection occurred upstream from the column by a micro-dosing pump. Two experiments were carried out with a 10-fold increase of metal concentrations, in order to cover the full range of operating conditions: Ni concentration from 10^{-4} (experiment 1) to 10^{-5} mol/L (experiment 2).

Column tests

The experimental setup is illustrated in Figure 1. The experimental setup consisted of a feed tank containing a boron/lithium solution with nitrogen sparging and a column filled with a mixed-bed ion-exchange resin (IRN9882, see below). The column dimensions were 2.6 cm in inner diameter for a 35-cm height of packed bed resins. Dissolved nickel, cobalt and silver were injected into the column in different concentrations. The column was fed from the top to the bottom by a stock solution contained in a tank with a capacity of 550 L. The average volumetric flow rate was within the range 25.5 – 27.5 L/h. The tests were performed at room temperature.

The global volume of percolating fluid is about several cubic meters taking into account the mass of nickel required for saturating the resin, the amount of resin contained in the column and its exchange capacity. Therefore, the solutions that had percolated through the packed column of mixed bed resin were reconditioned by passing through a mixed-bed IRN160 resin, which was preconditioned in borate and lithium for the anionic and cationic components, respectively. This circulation system allowed:

- to remove metals from the circulating solution, and to prevent them from polluting the tank;
- to restore the solution concentrations in boron and lithium, which had been fixed in the packed resin column;
- to fix the H^+ ions, released in solution consequently to nickel exchange, by the IRN160 reconditioning resin;
- to remove the sulfate ions from the circulating solution.

Conductivity monitoring and regular sampling for chemical analysis of the solutions at the column inlet led to the following observations:

- the residual background concentrations in nickel, cobalt and silver at the tank output were low with respect to the concentrations injected into the column;
- the boron concentration was stable and varied by less than 5% during a given test;
- the stability of the injected lithium concentration was maintained as long as the significant nickel breakthrough was not reached. Afterwards, the lithium concentration progressively increased up to 2.5 ppm.

Mixed-bed ion-exchange resins

A mixed-bed of strong acid/strong base macroporous resins (IRN9882) provided by Rohm & Haas was packed into the column. This resin was of nuclear grade, that is to say, it had undergone several washes in order to reduce the content of impurities. Table S1 summarizes the properties of the mixed-bed resin.

Multi-component reactive transport

Modeling of hydrodynamics and transport

OPTIPUR is a numerical tool for simulating the purification of aqueous solutions in the cooling systems of nuclear power plants by ionic exchange in packed bed resins. A packed bed of ion exchange resins can be decomposed in different zones: the advection dominated bulk solution, the Nernst film where mass transfer takes place mostly by diffusion and migration, and finally the resin beads, bearing the functional sites. This section summarizes the main equations implemented in the OPTIPUR code that govern the transfer of dissolved species into the packed bed resin column[6]. These equations are presented here with increasing complexity, taking into account more and more correctly the diffusion of ions in the Nernst layer adhering to the resin beads.

The simplest mode of transport in OPTIPUR was derived from the HYTEC[7] code and corresponds to the classical reactive transport equation based on advective/dispersive mass transfer. The exchange resin beads are assumed to be directly accessible to the ions flowing through the column:

$$\omega \frac{\partial C_i}{\partial t} = -Ugrad(C_i) + grad\big(Ddiv(C_i)\big) - \frac{\partial Q_i}{\partial t} \quad (1)$$

where ω represents the porosity of the resin bed, C_i the total concentration of an element in solution (mol/L or mol/m^3), U the flow velocity (m/s), D the dispersive/diffusive coefficient in the bulk (common to all ions, in m^2/s); $D = D_e + \alpha U$ with D_e the effective diffusion coefficient (m^2/s), negligible at fast flows, and α is the dispersivity (m). The resin volume and porosity are assumed to be constant: any swelling or shrinking due to ion exchange is neglected. The last term $-\frac{\partial Q_i}{\partial t}$ is the reaction-term induced by the (de)sorption of ions at chemical equilibrium with the resin(s).

Numerically, Equation 1 is solved for the column with a 1D finite volume approach. This equation is discretized in space by a first-order upstream spatial scheme for advection and by a second order centered spatial scheme for dispersion. The time discretization is a one-step implicit scheme. The reactive transport is based on a sequential iterative operator splitting method that allows a partial decoupling of the chemistry and transport equations. Within a single time-step, there is a cycle of iterations between transport and chemistry until convergence is reached. While Equation 1 holds for all solutes (with an additional reaction term), it is only solved for the total concentrations of the basis components, as usual in reactive transport modeling[7].

However, the hypothesis of equilibrium between the resins and the bulk solution is not realistic in the present case, and leads to extremely sharp exchange fronts for divalent ions. The second and third transport modes explicitly take into account the difference in solution composition in the column void volume (bulk solution) and at the resin interface (where only negligible accumulation takes place in the aqueous phase):

$$\begin{aligned} \omega \frac{\partial C_{i,Bulk}}{\partial t} &= -Ugrad\big(C_{i,Bulk}\big) + grad\left(Ddiv\big(C_{i,Bulk}\big)\right) + a_s(1-\omega)J_{C_i} \\ \frac{\partial Q_i}{\partial t} &= -a_s(1-\omega)J_{C_i} \end{aligned} \quad (2)$$

where J_{C_i} (mol/s) represents the exchange flux between the bulk and the close neighborhood of the resin particle, it allows to take into account the film kinetics. The specific surface area a_s (m^2/m^3) is the ratio between the surface and the volume of the resin particle. As resin particles are supposed to be spherical of diameter d_p, $a_s = \frac{6}{d_p}$.

The second mode, hereinafter denoted as "mass transfer coefficient" or MTC, greatly simplifies this flux by setting it proportional to the concentration difference:

$$J_{C_i} = k\left(C_{i,Interface} - C_{i,Bulk}\right) \quad (3)$$

where k is a mass transfer coefficient common to all ions (expressed as a velocity dimension in m/s).

The third mode, hereinafter denoted as "Nernst-Planck", takes into account different diffusion coefficients at infinite dilution D_i^∞ (m^2/s) for each solute i (exchangeable ions, co-ions and neutral molecules) in the Nernst layer as well as an electric potential field gradient to maintain the electroneutrality balance within the Nernst layer, namely:

$$J_i = -D_i^\infty \left(grad[C_i] + \frac{z_i[C_i]F}{RT} grad\Phi\right) \quad (4)$$

The term z_i is the ion charge, F and R are the Faraday and ideal gas constants, Φ stands for the electric potential (V). In all cases, the ions in contact with the outer surface of the resin beads are considered to instantly penetrate inside the bead without any internal transport kinetics. With the hypothesis that concentration profiles are linear within the Nernst film of thickness δ (m), we can define an effective diffusion coefficient for each solute:

$$D_i = \frac{J_i \delta}{C_{i,Resin} - C_{i,Bulk}} \quad (5)$$

Several limiting behaviors can be derived from Equation 5. In the absence of electric field, D_i is equal to D_i^{∞}, the infinite dilution diffusion coefficient, and the transport across the Nernst film is purely diffusive. When the transport is pure migration, the effective diffusion coefficient diverges because the denominator collapses. The electric field can cause the flux to be against the concentration gradient. In such a case, D_i takes negative values. Finally, when there is no transport across the Nernst film, the effective diffusion coefficient is equal to zero.

The thickness of the Nernst film is considered to be the same of all species and is estimated from correlations between the dimensionless Reynolds, Schmidt and Sherwood numbers. Following the approach described by Franzreb *et al.*[8] and Jia *et al.*[4] , OPTIPUR estimates, in the general case of multi-component diffusion, a mean diffusion coefficient:

$$D_r = \frac{\sum |J_i| \delta}{\sum |C_{i,bulk} - C_{i,resin}|} \quad (6)$$

The summation is over all mobile species in solution, D_r is the overall diffusion coefficient (m^2/s), δ is the average thickness of the Nernst layer (m), C_i^{bulk} and C_i^{resin} are respectively the concentrations of each mobile species in the bulk solution or at the resin interface. In other words, D_r is the harmonic mean of the absolute value of effective diffusion coefficients, weighted by the absolute value of the flux.

The Nernst film thickness is finally estimated through the correlations of Wakao and Funazkri[9], Equation 7, or Dwiveidi and Upadhyay[10], rewritten in the form of Equation 8.

$$\frac{d_p}{\delta} = 2 + 1.1 Sc^{1/3} Re^{0.6} \quad (7)$$

$$k = \frac{D_r}{\delta} = \frac{D_r}{d_p} Sc^{1/3} Re \left[\frac{0.765}{(\omega Re)^{0.82}} + \frac{0.365}{(\omega Re)^{0.386}} \right] \quad (8)$$

Here, d_p is the average diameter of the resin beads (m), S_c and R_e are the Schmidt and particle Reynolds numbers, respectively. Since mixed beds are considered in this study, two resin interfaces are handled and a representative diffusion and Nernst film thickness is calculated for each.

Modeling of water chemistry

The local thermodynamic equilibrium is solved according to mass balance equation of total concentration and the methods of basis components based on the law of mass action:

$$K = \frac{(C)^{n_c} (D)^{n_d}}{(A)^{n_a} (B)^{n_b}} = e^{\left(\frac{-\Delta_r G^0}{RT}\right)} \quad (9)$$

where the brackets correspond to the activity of the species, K and $\Delta_r G^0$ are respectively the equilibrium constant and the standard free energy (1 atm, 25 °C) characteristic of the chemical reaction. In the basis component formalism[7], chemically independent basis species are chosen, in such way that all the derivative species, aqueous complexes or sorption sites, can be expressed with these basis species.

The empirical formula of the truncated Davies model, derived from the physico-chemical Debye-Huckel model, was considered in this study. It is applicable for low to moderately mineralized solutions (i.e. ionic strength less than 0.5).

Modeling of ionic exchange

In the present conditions of pollutants at low concentrations and resins with strong exchange capacity, the limiting step is the diffusion through the Nernst film and not the kinetics of the exchange reactions or the diffusion of ions in the resin beads. The exchange reaction, between an ion B^{2+} (e.g. Co^{2+}) from

the injection solution and two exchangeable ions A^+ (e.g. H^+) from the resin, is also described by a law of mass action at thermodynamic equilibrium as follows:

$$2\overline{A^+} + B^{2+} \rightleftharpoons \overline{B^{2+}} + 2A^+, K = \frac{\left(\overline{B^{2+}}\right)(A^+)^2}{\left(\overline{A^+}\right)^2 (B^{2+})} \quad (10)$$

OPTIPUR deals with different formalisms of ion activity fixed into the resin. This study uses Vanselow's formalism where the activity of an ion bound to the resin is calculated on the mole fraction scale. In the case of Equation 10, the activity of the B^{2+} ion in the resin phase is considered to be equal to the mole fraction of B^{2+}, $f_{B^{2+}}$, which can be written in case of a binary exchange as:

$$f_{B^{2+}} = \frac{[\overline{B^{2+}}]}{[\overline{A^+}] + [\overline{B^{2+}}]} \quad (11)$$

where the square brackets represent concentrations in mole per liter of solution or mole per gram of resin. Non idealities in the resin phase were not taken into account in this study.

Modeling parameters

The geometrical and hydrodynamic parameters used in the modeling are reported in Table S2. Both the anionic (60% by volume) and cationic (40%) resins of the mixed-bed column were considered in the modeling. The solution chemistry (acid/base and complexation processes) was calculated at equilibrium according to the EQ3/6 thermodynamic database[11] at 25°C. In order to account for the formation of polyborates in the bulk solution, the formation constants of Palmer *et al.*[12] for the mono, di and tri-borate ions at 25°C were added to the database in place of BO_2^- ion from EQ3/6. The formation constant of complexes of nickel and cobalt with boric acid were estimated from the measurements of Shchigol[13], but following the review of Gamsjäger *et al.*[14] that suggests the formation of neutral borato complexes.

Ion exchange resins are characterized by several parameters like exchange capacity and selectivity coefficient. Exchange capacity is defined as the number of functional groups within the resin, i.e. the number of counter-ions in a specified amount of the materials. Selectivity coefficient gives an assessment of resins relative affinity. Table S3 gives the ion exchange capacity and selectivity coefficients used in modeling the ion exchange equilibrium according to Equation 10 for the cationic and anionic components. Bonner and Smith[15] have published selectivity constants for synthetic resins with DVB percentage between 10% and 16% (the cationic part of IRN9982 consisting of 12% DVB). Gressier[16] has derived from specific experiments the selectivity coefficients of the resin IRN9882. Lou *et al.*[17] have proposed a model for the sorption capacity of boron on an anionic exchange resin. However, this model is not compatible with the framework of reactive transport modeling used here. Selectivity coefficients for (poly)-borates were therefore estimated empirically to reproduce the observed apparent capacity (more than one boron atom per exchange site). As a literature value could not be found, the selectivity coefficient for sulfate was arbitrarily set to 10. However, because divalent sulfate easily remove monovalent anions from the resin, this value should not have a large impact on the results. The resin exchange capacities are assumed to be constant in time. The diffusion coefficients D_i^∞ used in the Nernst-Planck modeling (Equation 4) and the formation constant of derived species are given in Table S4 for the all species in solution. The correlation of Wakao and Funazkri was used unless otherwise specified to estimate the film thickness.

Preliminary modeling results

Profile of exchangeable species inside the column

OPTIPUR calculates the chemical equilibrium between the mobile and stationary phases but also the elution fronts for each ion at any time. The ability to analyze the chemistry evolution inside the column is an advantage of the modeling approach, compared to experiment where it is often difficult to get such an observation.

Under the chemical conditions inside the column (in particular a pH around 6), the free species Ni^{2+}, Co^{2+}, Li^{+} and Ag^{+} account for more than 99% of the total metal concentrations, even when complexes with sulfate or borate anions are taken into account. This suggests that the water chemistry can be simplified by neglecting these complexes. However, since the computational cost of including them in the calculation is negligible thanks to the reactive transport approach were only basis species are transported, they were generally considered, unless otherwise specified. The chromatographic fronts of the monovalent cations Ag^{+} and Li^{+} are sharp, as shown in Figure 2a after 10 hours for experiment 1. These elements are pushed forward by the divalent cations Ni^{2+} and Co^{2+} of higher affinity for the resin, thereby resulting downstream in breakthrough concentrations of monovalent cations above their initial concentrations (Figure 3).

In the case of anions, there is a progressive but complete exchange between $B(OH)_4^-$ (and poly-borates) and the sulfates SO_4^{2-} (Figure 2b). It is worth mentioning that calculations made with and without anion exchange have demonstrated that the elution of cations was little influenced by anion exchange, probably because sulfate and borate are exchanged downstream from the cation exchange fronts. Therefore, in the following, the paper will focus on the mobility of the metallic cations only.

Experiment 1, the base case

Constant mass-transfer coefficient modeling

Two types of simulations were performed with OPTIPUR. The first ones used the mass transfer mode by which the mass transfer coefficient (MTC) is fitted from the experiments according to the formula given by Hussey and Foutch[18]:

$$\mathrm{MTC} = -\left(\frac{1}{6\,(1-\omega)\,R_i}\right)\frac{u}{Z}\,d_p \ln\left(\frac{C}{C_0}\right) \tag{12}$$

where R_i is ratio of the volume of cationic resin to the volume of anionic resin in the mixed bed ($R_i = 1$ for an unmixed bed), u is the filter velocity (m/s), Z is the depth of the resin bed (m), d_p is the mean diameter of the resin beads (m), C is the outlet concentration and C_0 is the inlet concentration (injection solution).

In the case of experiment 1, the MTC value was adjusted to 6×10^{-5} m/s to fit the initial nickel leakage. The breakthrough curves of nickel, cobalt and silver calculated accordingly are shown in Figure 3(inset). The modeling/experiment agreement is globally good for nickel since the adjustment has been made for this metal, although saturation is reached sooner in the modeling. The agreement is fair for silver, in particular regarding the maximum concentration peak. However, the outlet silver concentration increases earlier in the calculations than in the experiment. The agreement is only fair for cobalt. The hierarchy of the chromatographic processes is globally well reproduced by the modeling. Silver is pushed forward (eluted) by the nickel front leading to a maximum concentration three times higher than the injection concentration. Divalent ions generally present a higher affinity for the resin than monovalent ions. Indeed, mathematically, though the absolute value of the selectivity constant of silver ($K_{Ag/H}$ = 10.0, Table S3) is greater than the constant for nickel ($K_{Ni/H}$ = 3.0), the aqueous and fixed concentrations of silver are squared in Equation 10 for the nickel/silver exchange. The selectivity constant of cobalt ($K_{Co/H}$ = 2.6) is slightly lower than the nickel one, which also results in the modeling in a breakthrough concentration of cobalt higher than the injected one (though more moderately than for silver). This process is more pronounced in the modeling than in the experiment where no significant enrichment in cobalt is observed.

Beside the breakthrough curves, one way to emphasize the processes at an early stage when the released concentrations are low is to draw the decontamination factor, $DF = log\left(\frac{C_0}{C}\right)$. A high factor means a strong retention of the metals by the resin. A factor tending to zero means that the resin has reached saturation with respect to a given metal. The decontamination factors, both experimental and calculated with the mass transfer mode, of the first experiment are shown in Figure 3. Despite the fact that the mass transfer coefficient was adjusted upon the initial leakage of nickel, the quality of modeling is also clearly good with respect to the decontamination factor of nickel and cobalt over the whole experiment.

Modeling underestimates the decontamination factor of silver, by up to one order of magnitude, until 18 hours.

Nernst-Planck modeling

The experimental data for mass transfer fitting are not always available. In that case, the Nernst-diffusion model allows running simulations in a more mechanistic manner. Because of the increased complexity, the computation time was about 7 times higher than in the MTC case. Figure 4 shows the corresponding breakthrough curves and decontamination factors. The calculated evolutions for cobalt and nickel are very similar to those obtained with the mass transfer mode. The silver peak is higher with the Nernst-Planck modeling than it was with the MTC modeling since silver, which is allowed to diffuse faster than nickel and cobalt, is more enriched. The decontamination factor for silver is closer to the experimental one, and is different from the nickel and cobalt ones. The agreement between modeling results and experimental values is remarkable, since no adjustable parameter was used in the model. The biggest differences between the experiment and Nernst-Planck modeling are when the resin gets saturated in nickel. The code again predicts an enrichment in cobalt, which is not seen in the measured concentrations, and a saturation that takes place earlier. The latter could be explained by an ion exchange capacity that is effectively higher than the manufacturer specification which was used in the modeling. But the absence of cobalt enrichment suggests a decrease in the resin affinity for nickel while saturation is approached, which would lead to both an increase in the time to reach saturation and the absence of cobalt enrichment.

The decrease in resin affinity could be caused by the formation of complexes of nickel in the bulk solution when the nickel concentration is high. The available complexation constants for nickel and sulfate were included in the reaction database, but no significant complex formation is predicted to take place. Soluble nickel borate and cobalt borato complexes can also be formed, but the recent review[14] pointed out that the dissociation constant reported in the literature may not be correct due to misinterpretation of experimental data. However, the experiments of Shchigol[13] suggest that no significant complexation of nickel and cobalt should take place at the relatively low concentration of nickel used in this study. Including complexes of nickel and cobalt with borates that fit Shchigol's experimental data into the calculation did not lead to any significant modification of the breakthrough curves. Another explanation of the decrease in affinity could be the variation of selectivity coefficients with the loading of the resin, which is firmly established[16], but unfortunately not quantified in the experimental conditions used here.

Figure 5a plots the average mass transfer coefficient calculated at the outlet of the column from the Nernst-Planck modeling according to the empirical correlation of Wakao and Funazkri (Equation 7), for the cation-exchange resin, with complexes of nickel and cobalt with sulfate and borate ions excluded for simplicity. The value of the coefficient is calculated from Equations 6 and 7 and is dependent on the evolution of the column chemistry, more specifically on which exchange takes place. The value of the average mass transfer coefficient at the beginning of the experiment is totally consistent with the value used for the MTC modeling. Figure 5b plots the ratio of the effective diffusion coefficients as defined by Equation 5 to the infinite dilution diffusion coefficient for different ions, as a function of time, at the interface between the bulk solution and the cation exchange resin at the column outlet.

After a few minutes of experiment, the anion exchange resin is saturated with boron and the bulk aqueous solution at the column outlet is composed of boric acid at the inlet concentration and traces of the other elements. At the resin interface, the concentrations of Li^+, Ag^+, Ni^{2+} and Co^{2+} are at equilibrium with the resin and much lower than in the bulk solution. Thus Li^+, Ag^+, Ni^{2+} and Co^{2+} are transported at small concentrations towards the resin, and H^+ in the other direction. The different mobility of these cations are compensated by the concentration of co-ions, mainly $B(OH)_4^-$, since the concentration of SO_4^{2-} is very low. As described by Helfferich[2], with the faster ion initially in the ion exchange, the concentration of co-ions will be lower at the bulk interface than in the bulk solution and the ions coming into the resin will be accelerated, while the protons will be slowed down. This is apparent from figure 5b, since the plotted ratios at the beginning of the experiment are slightly above 1, indicating a small acceleration for Li^+, Ag^+, Ni^{2+} and Co^{2+}, while much lower than 1 for H^+ ions. The

ratio is equal to 0 for sulfate ions, which indicates that the diffusion is exactly compensated by the migration and is consistent with the exclusion of co-ions from the exchanger phase. However, the ratio for borates is not zero, and is almost equal to the ratio for H^+ ions. This is because the two fluxes are coupled by the dissociation of boric acid, which bears no electrical charge and diffuses without being affected by the electric field. In fact, the more concentrated species are more affected by the electric field. As ion exchange takes place, the concentration of first sulfate and later lithium at the column outlet increases, and as a result the intensity of the electric field increases, up to a maximum around 9 h and decreases to almost zero at 14 h. When the concentration difference for Li^+ across the interface vanishes, the apparent diffusion coefficient of lithium diverges, since the denominator tends to zero and changes sign. After that, lithium ions electro-diffusing out of the resin are slowed down by the effect of the electric field and their diffusion coefficient becomes lower than its infinite dilution value. The same behavior as lithium is predicted for the diffusion coefficient of Ag^+ and Co^{2+} ions, which both have a peak in their breakthrough curves. Finally, after 25 h, the main remaining ion exchange reaction is the exchange of Co^{2+} ions at trace levels for Ni^{2+} ions. Since cobalt is slightly slower than nickel, the electric field is in the opposite direction, slowing down nickel ions. The diffusion coefficient of Ni^{2+} and Co^{2+} is very close to the infinite dilution value, while that of SO_4^{2-} ions is higher than the infinite dilution value, indicating in this situation that the difference in mobility of the exchanging cations is compensated by a net flux of co-ions.

Specific conductivity

The evolution of the specific conductivity as a function of time can be calculated by the code. This value that is easily measured experimentally allows for quick assessment of the experiment/modeling agreement. Figure 6 shows the experimental and calculated conductivity for the first experiment. The agreement is good, but the specific conductivity before 10 hours may be slightly overestimated. However, since the temperature of the experiment was not carefully controlled, such a difference remains within the estimated experimental uncertainty. The poor knowledge of the contribution of polyborates to conductivity may also explain this difference.

The slight but constant increase in the experimental conductivity after 30 hours is due to the contamination of the stock solution by lithium as discussed above. The closed loop and its later experimental artifact were not introduced in the modeling.

Sensitivity of breakthrough curves vs. bead diameters and correlation

The size of the resin beads may have an influence on the contact surface and mass transfer between the bead and the flowing fluid, but also on fluid flow through the column. The IRN9882 resin shows a distribution of particle size between 0.4 and 1.0 mm. OPTIPUR can only take into account a single particle size. Figure 7 shows the effect of the cation exchange resin bead diameter on the breakthrough curve of silver with the Nernst-Planck modeling. The bead diameter has an influence on both the silver peak height and time, and also on the initial decontamination factor. Different correlations can be used to estimate the Nernst film thickness. Figure 8 shows the effect of the correlation used on the breakthrough curves of nickel and silver. The correlation of Dwiviedi and Upadhyay leads to a silver peak that is high, comes early and produces high decontamination factors. The correlation of Wakao and Funazkri leads to results in better agreement with the experimental data. However, the present experiment with resin beads of non uniform diameter may not lead to definitive conclusions on which correlation should be used.

Experiment 2, a factor 10 decrease in metal concentrations

Constant mass-transfer coefficient modeling

Compared to the first experiment, the time required to saturate the resin in experiment 2 should be increased proportionally to the factor 10 decrease in metal concentrations. This is not totally the case here since the saturation times for nickel are about 24 hours versus 220 hours in experiment 1 (Figure 3) and experiment 2 (Figure 9), respectively. The earlier saturation in experiment 2 is due to the higher mean value of the volumetric flow rate, that is to say 27.5 L/h in experiment 2 versus 25.8 L/h during experiment 1. The experimental data of cobalt and silver before 100 hours were below the detection

limit (10 µg/L). Fitting of the mass transfer factor on the breakthrough curve of nickel according to Equation 12 gives a mass transfer coefficient of 6×10^{-5} m/s, similar with the factor derived from experience 1.

Figure 9 shows the results of the calculation with a constant mass transfer coefficient. The agreement of the simulated concentrations with the measured ones is very good for nickel, cobalt and silver. Like in experiment 1, a temporary enrichment in cobalt is predicted, but not observed. The decontamination factor of nickel during the whole experiment is well modeled, even though the mass transfer coefficient was fitted only to the initial nickel leakage. The silver concentration is predicted to be higher than the detection limit after about 1 day, whereas it was the case only after 100 h. The decontamination factor for silver is thus probably underestimated by the MTC modeling.

Nernst-Planck modeling

The computation time was increased tenfold compared to the MTC case. The direct calculation of the diffusion of the ions in the Nernst layer gives modeling results that are globally in good agreement with the experimental data, without any parameter fitting. The experiment/modeling agreement is reasonably good for cobalt and nickel, both for the breakthrough curve and the decontamination factor (Figure 10). The silver concentration is predicted to reach the detection limit after 3 days, which is closer to the experimental value. The decontamination factor for silver in the beginning of the experiment may still be slightly underestimated.

Conclusion

A series of experiments in columns submitted to high flow rates have been modeled with the OPTIPUR code that simulates the ultra-purification of fluids by mixed-bed ion exchange resin. The chemistry of the fluid is composed of a mixture boron and lithium hydroxides with an addition of metal contaminant at low concentrations. One of the challenges of the modeling is its ability to capture both the breakthrough curves of the metal close to saturation as well as the early leakage related to the greatest decontamination factors.

Two methods of progressive complexity have been compared to model the film diffusion limitation. The first one needs to adjust *a posteriori* the mass transfer coefficient on the experimental breakthrough curves. Furthermore, a single common coefficient has to be assigned to the whole set of metals although the transfer may be metal specific. The second method is based on *a priori* mechanistic modeling of the species diffusion through the bead film by the Nernst-Planck equation, at the cost of a tenfold increase in computation time. The diffusion coefficient is ion specific, albeit the species fluxes are coupled to each other through electrostatic potentials.

The agreement between the experimental and modeling results is fairly good in all cases, in particular the chromatographic elution of silver by nickel and the subsequent enrichment of the solution in the former metal. A similar but much lower enrichment is forecast for cobalt in direct relation with the relative affinity (selectivity coefficient) of nickel and cobalt. This has not been observed in the experiments. The mass transfer approach was calibrated on the initial leakage of nickel and correctly reproduces the complete elution curve for nickel, but probably underestimates significantly the decontamination factor for silver. The Nernst-Planck approach produces results that are as good as the constant mass transfer approach or better, even though no fitting parameter was used. The latter approach should therefore be preferred in modeling film mass transfer limited ion exchange.

Aknowledgements

The constructive and detailed comments of three anonymous reviewers are greatly acknowledged.

Supporting information available

The supporting information includes the characteristics of the mixed bed resin used in this study, the detailed column properties, the list of selectivity coefficients used for the calculations as well as the

complete list of species, with associated diffusion coefficients and formation constants. This information is available free of charge via the Internet at http://pubs.acs.org

Literature Cited

(1) Gilliland, E. R.; Baddour, R. F. Rate of Ion Exchange. *Ind. Eng. Chem.* **1953**, *45*, 330.
(2) Helfferich, F. G. *Ion Exchange*; Dover Publications: Mineola, New York, 1995.
(3) Chowdiah, V. N.; Foutch, G. L.; Lee, G.-C. Binary Liquid-Phase Mass Transport in Mixed-Bed Ion Exchange at Low Solute Concentration. *Ind. Eng. Chem. Res.* **2003**, *42*, 1485.
(4) Jia, Y.; Foutch, G. L. True Multi-Component Mixed-Bed Ion-Exchange Modeling. *React. Funct. Polym.* **2004**, *60*, 121.
(5) Roth, D. W. H. Ternary Ion Exchange in Fixed Beds: Equilibrium and Dynamics. Ph. D. dissertation, New Jersey Institute of Technology: Newark, NJ, 1985.
(6) De Dieuleveult, C.; Lagneau, V. *OPTIPUR Logiciel de Simulation de Circuit D'épuration D'eaux - Documentation Technique*; Rapport technique R120825CDIE; MINES Paristech - ARMINES: Fontainebleau, 2013.
(7) Van der Lee, J.; De Windt, L.; Lagneau, V.; Goblet, P. Module-Oriented Modeling of Reactive Transport with HYTEC. *Comput. Geosci.* **2003**, *29*, 265.
(8) Franzreb, M.; Höll, W. H.; Sontheimer, H. Liquid-Phase Mass Transfer in Multi-Component Ion Exchange I. Systems without Chemical Reactions in the Film. *React. Polym.* **1993**, *21*, 117.
(9) Wakao, N.; Funazkri, T. Effect of Fluid Dispersion Coefficients on Particle-to-Fluid Mass Transfer Coefficients in Packed Beds: Correlation of Sherwood Numbers. *Chem. Eng. Sci.* **1978**, *33*, 1375.
(10) Dwivedi, P. N.; Upadhyay, S. N. Particle-Fluid Mass Transfer in Fixed and Fluidized Beds. *Ind. Eng. Chem. Process Des. Dev.* **1977**, *16*, 157.
(11) Wolery, T. J. *EQ3/6: A Software Package for Geochemical Modeling of Aqueous Systems: Package Overview and Installation Guide (version 7.0)*; UCRL-MA-110662 PT I; Lawrence Livermore National Laboratory: Livermore, CA, 1992.
(12) Palmer, D. A.; Benezeth, P.; Wesolowski, D. J. Boric Acid Hydrolysis: A New Look at the Available Data. *Power Plant Chem.* **2000**, *2*, 261.
(13) Shchigol, M. B. Properties of Cobalt and Nickel Borates. *Russ. J. Inorg. Chem.* **1961**, *6*, 1361.
(14) Gamsjäger, H.; Bugajski, J.; Gajda, T.; Lemire, R. J.; Preis, W. *Chemical Thermodynamics of Nickel*; Chemical thermodynamics; Elsevier: Amsterdam, 2005.
(15) Bonner, O. D.; Smith, L. L. A Selectivity Scale for Some Divalent Cations on Dowex 50. *J. Phys. Chem.* **1957**, *61*, 326.
(16) Gressier, F. Etude de La Rétention Des Radionucléides Dans Les Résines Échangeuses D'ions Des Circuits D'une Centrale Nucléaire À Eau Sous Pression. Ph. D. dissertation, Mines ParisTech: Paris, 2008.
(17) Lou, J.; Foutch, G. L.; Na, J. W. The Sorption Capacity of Boron on Anionic-Exchange Resin. *Sep. Sci. Technol.* **1999**, *34*, 2923.
(18) Hussey, D. F.; Foutch, G. L. Ion-Exchange Kinetics for Ultrapure Water. In; SenGupta, A. K.; Marcus, Y., Eds.; Ion Exchange and Solvent Extraction; Marcel Dekker: New York, 2004; pp. 339–373.

Table 1. Experiments 1 and 2: water chemistry, metal concentrations, duration and flow rate.

Test	Exp. 1	Exp. 2
pH	5.5	5.2
B (mg/L)	2645	2880
Li (mg/L)	1.2 – 2.2	0.75 – 1.4
Ni (mol/L)	1.4×10^{-4}	1.6×10^{-5}
Co (mol/L)	1.9×10^{-6}	2.5×10^{-7}
Ag (mol/L)	2.9×10^{-6}	3.1×10^{-7}
Mean volumetric flow rate (L/h)	25.8	27.5
Duration (h)	54	330

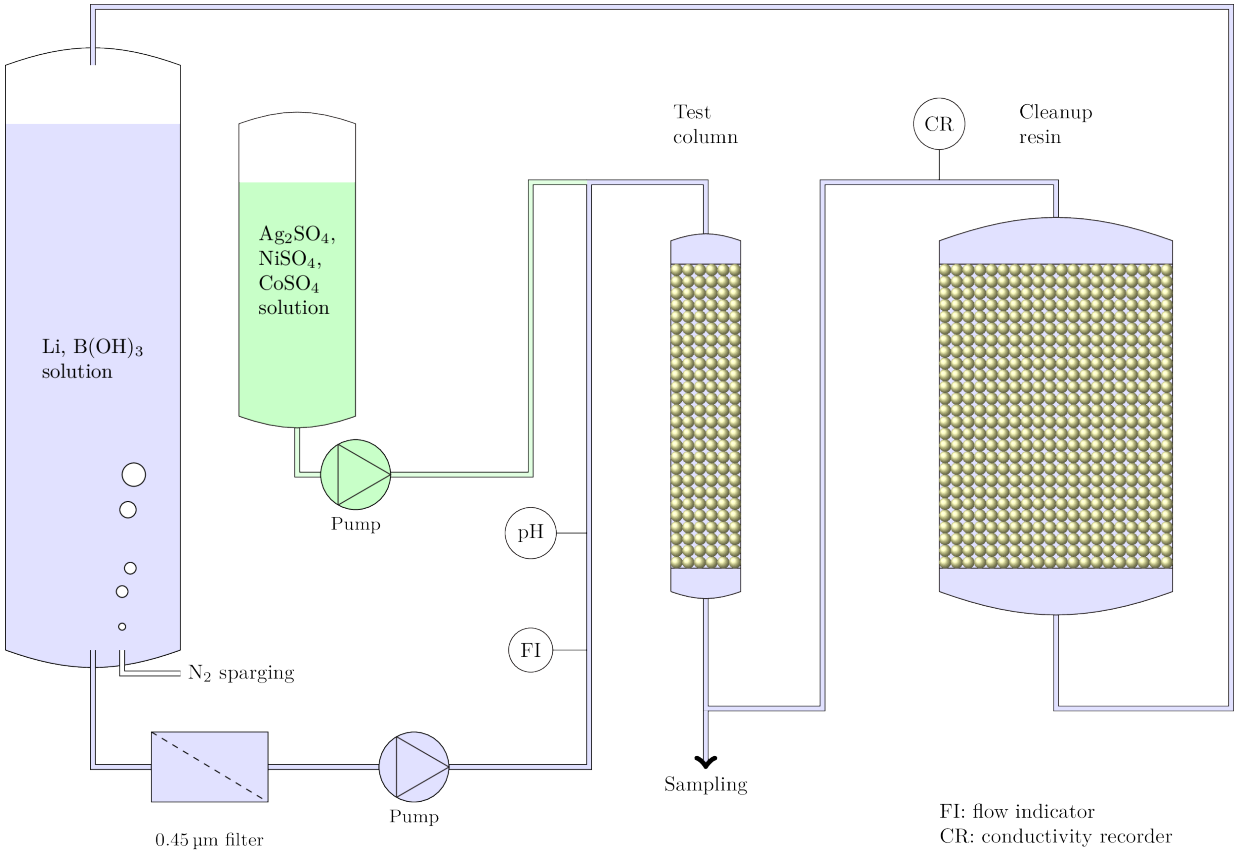

Figure 1. Experimental set-up.

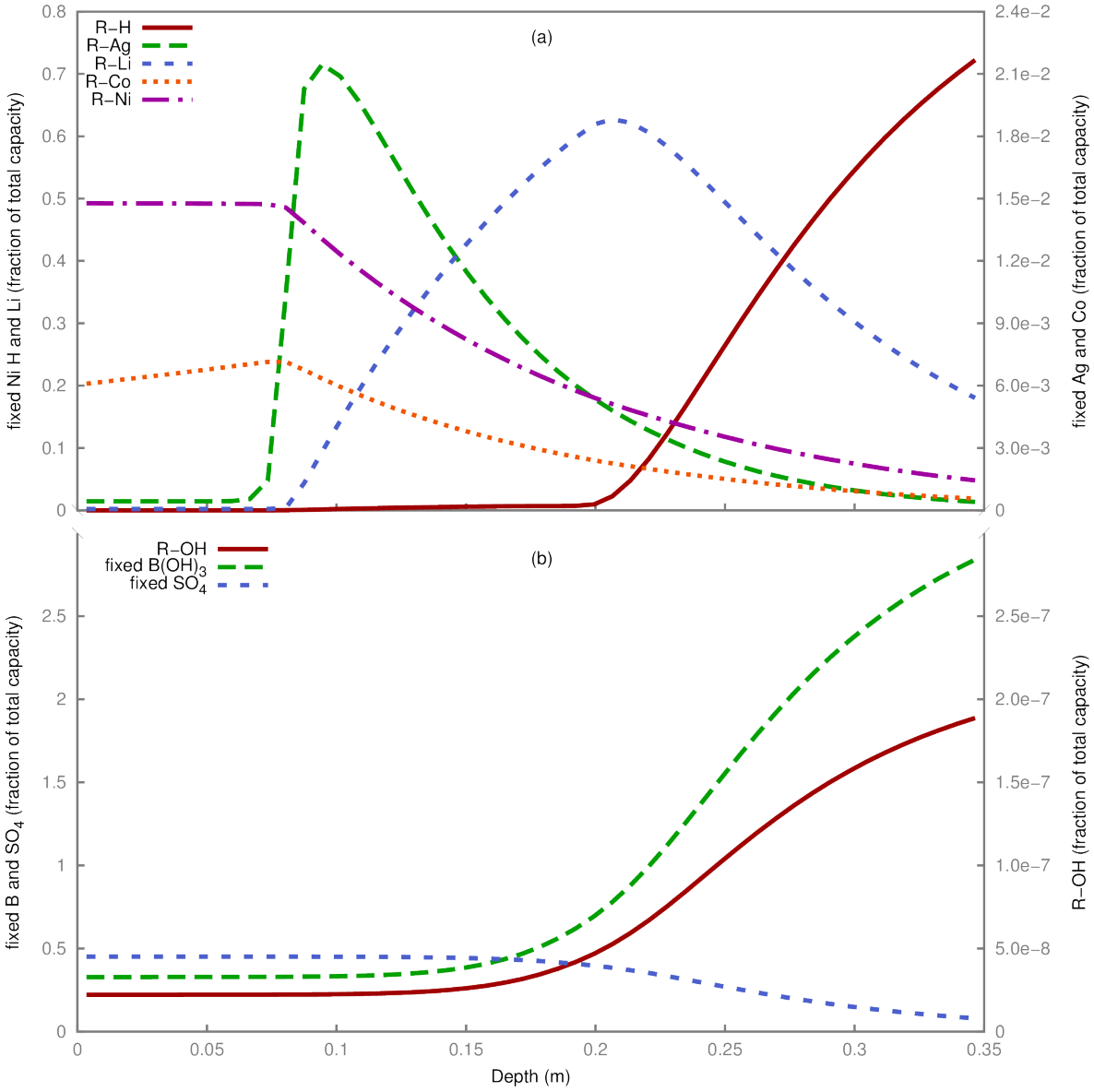

Figure 2. Experiment 1: calculated profiles of exchangeable cation (a) and anion (b) concentrations along the column after 10 hours.

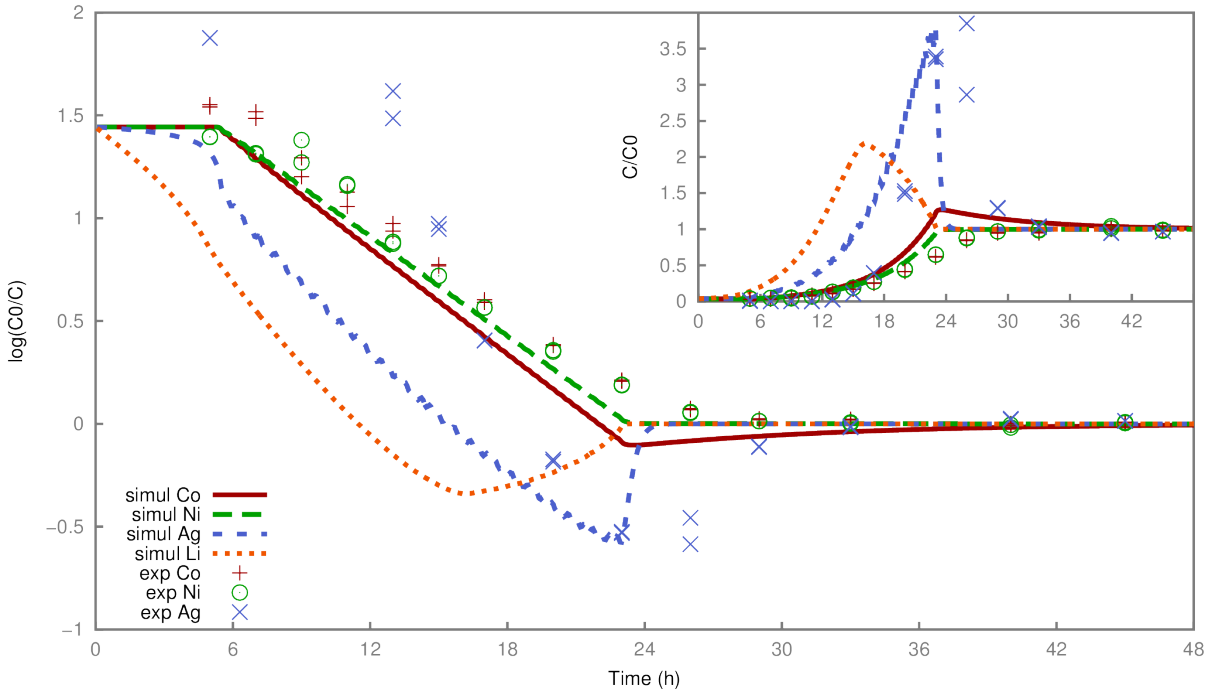

Figure 3. Experiment 1, comparison between experiment and modeling in the mass transfer coefficient (MTC) approach: decontamination factor and normalized breakthrough curve (inset).

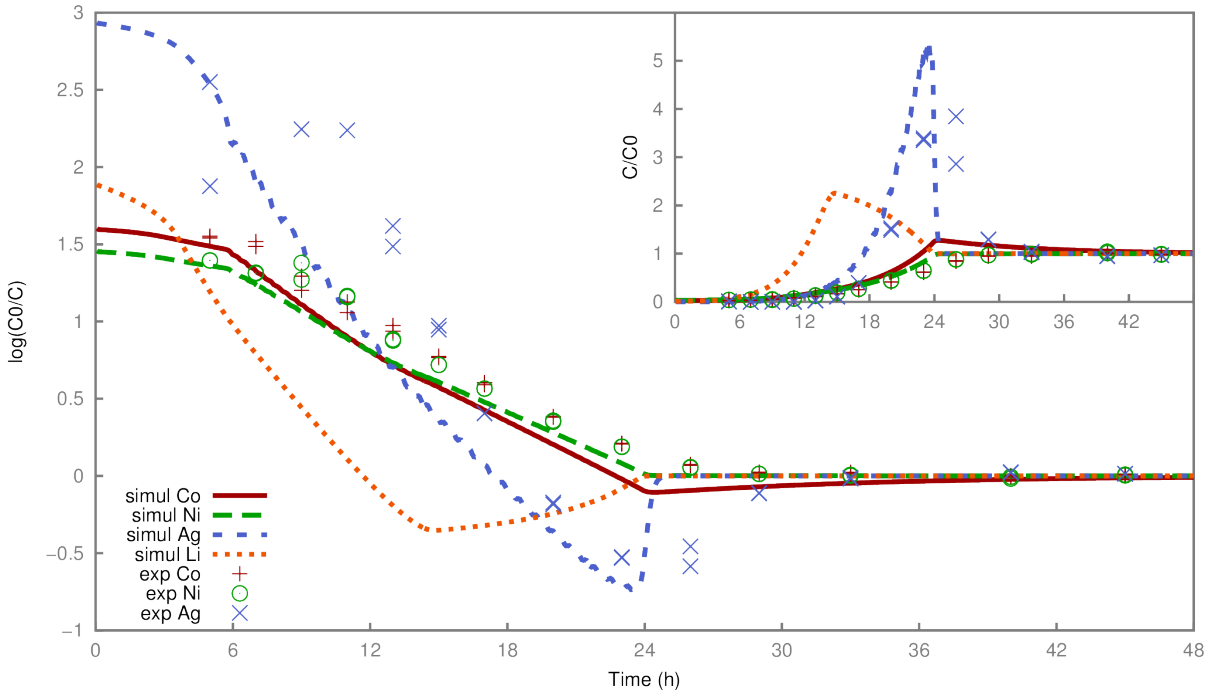

Figure 4. Experiment 1, comparison between experiment and modeling in the Nernst-Planck approach: decontamination factor and normalized breakthrough curve (inset).

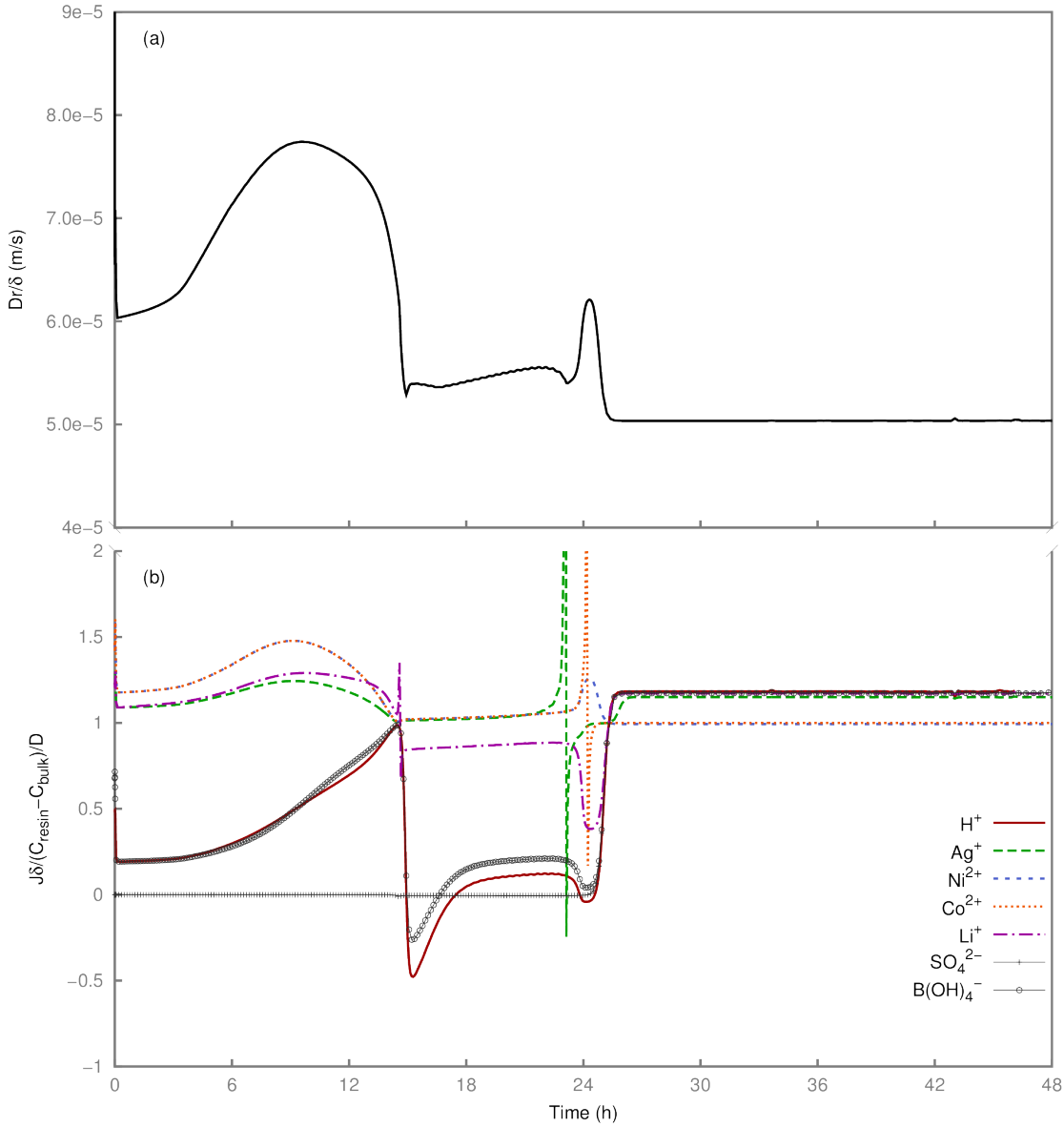

Figure 5. Experiment 1, modeling in the Nernst-Planck approach: evolution of the calculated average mass transfer coefficient (a) and effective diffusion coefficient for different ions (b).

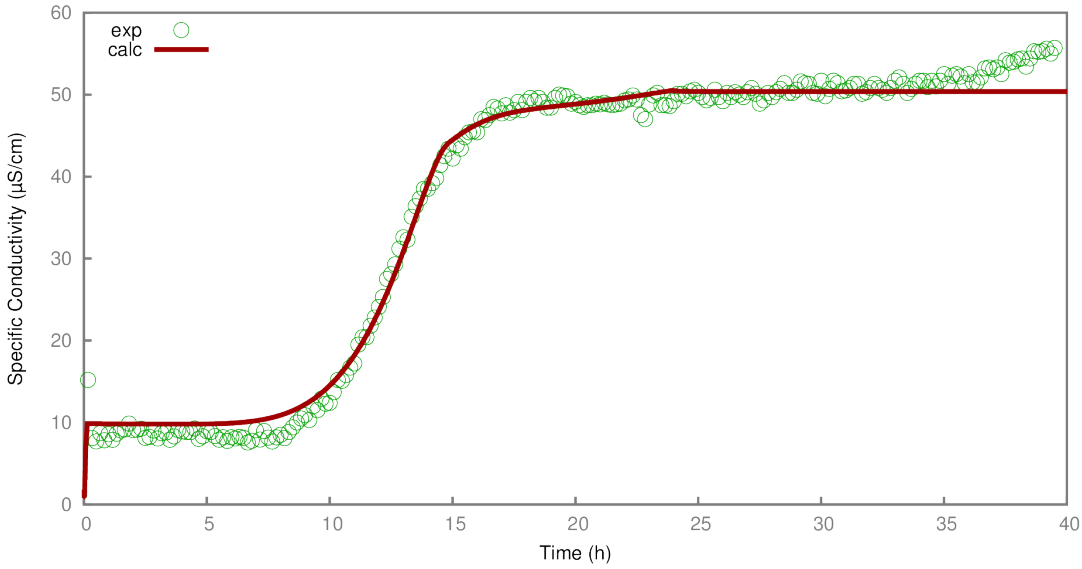

Figure 6. Experiment 1, comparison between experiment and modeling in the Nernst-Planck approach: electrical conductivity.

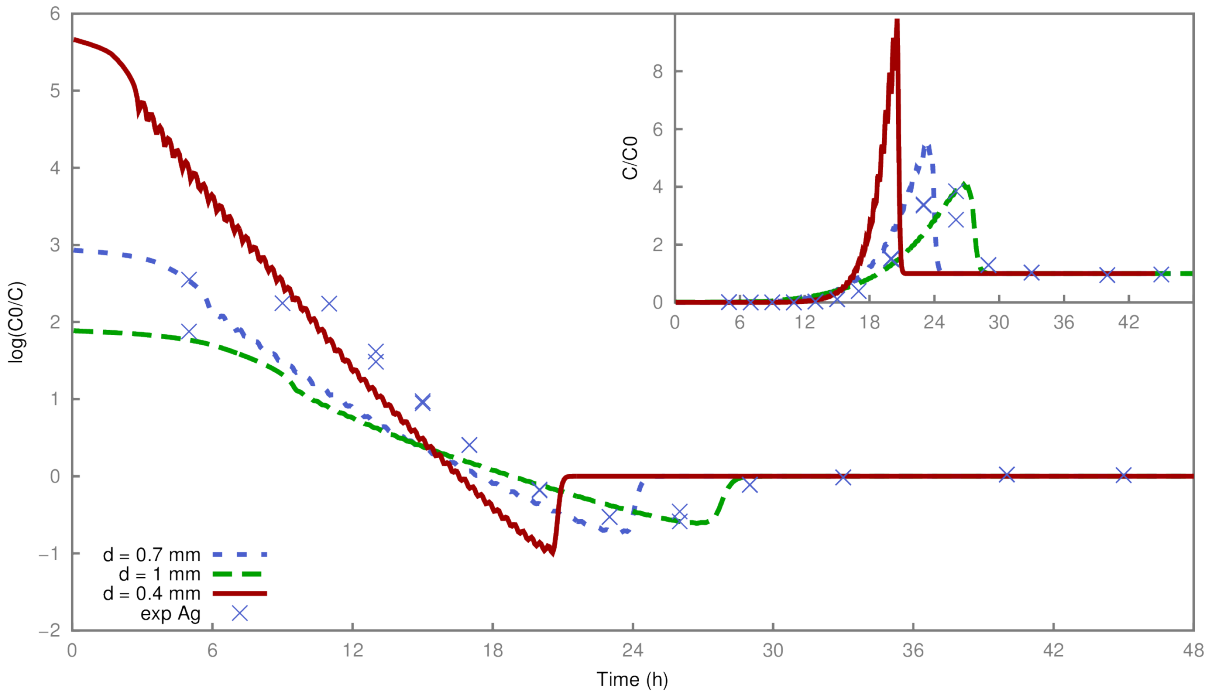

Figure 7. Experiment 1: modeling sensitivity of bead diameter effect on the decontamination factor of silver and normalized breakthrough curve (inset).

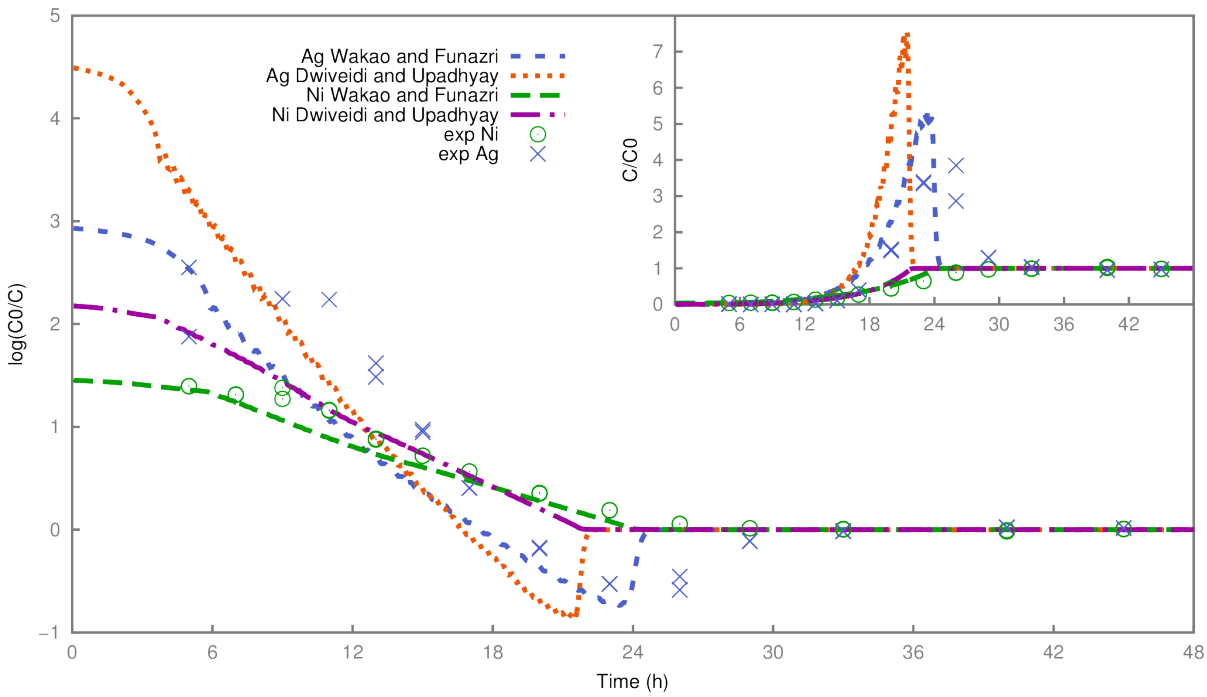

Figure 8. Experiment 1, sensitivity of the model to the correlation used to estimate the Nernst film thickness: decontamination factor for nickel and silver and normalized breakthrough curve (inset).

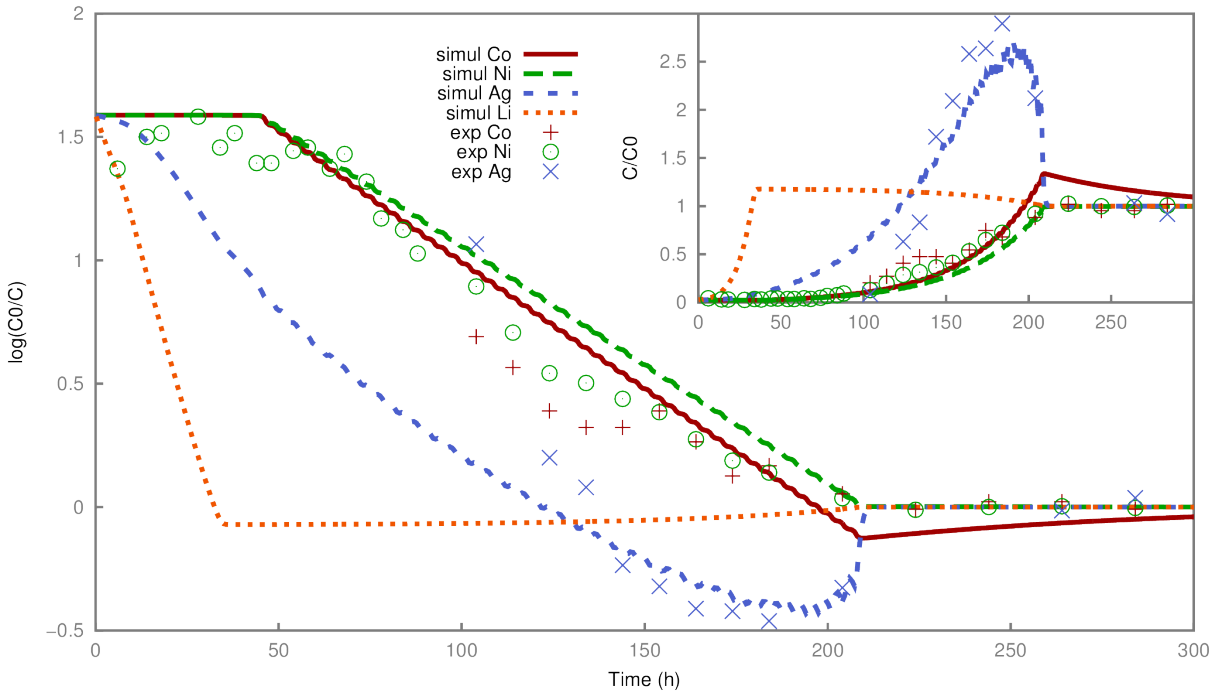

Figure 9. Experiment 2, comparison between experiment and modeling in the mass transfer coefficient (MTC) approach: decontamination factor and normalized breakthrough curve (inset).

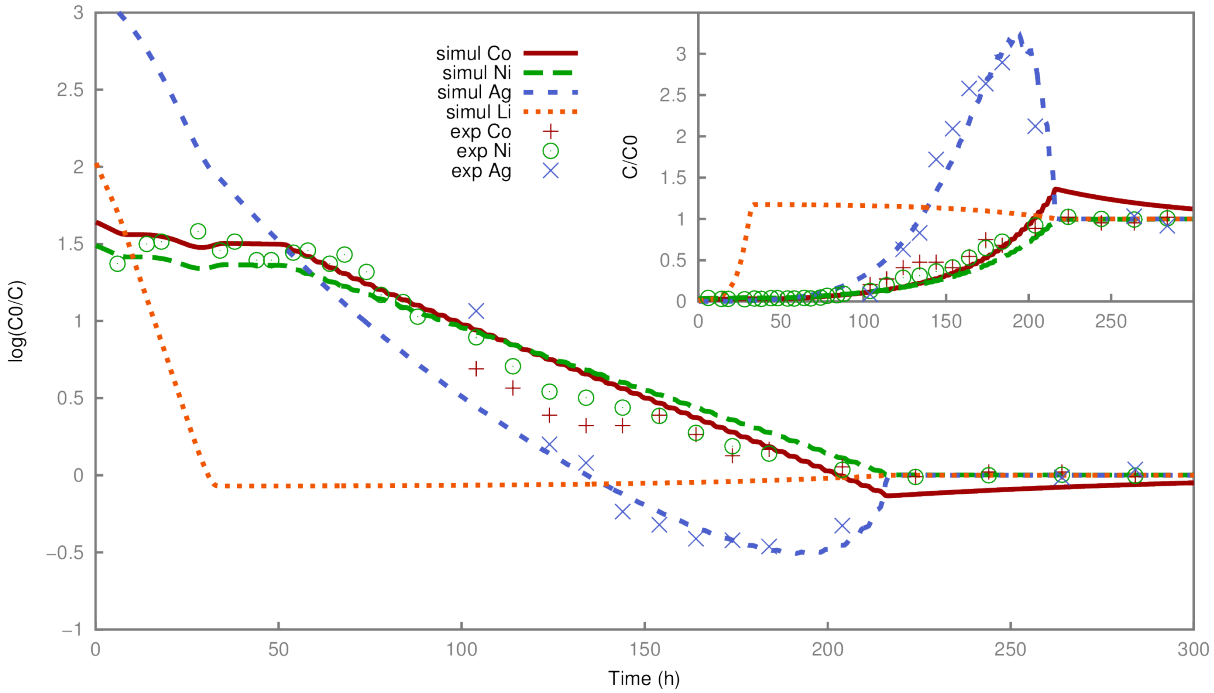

Figure 10. Experiment 2, comparison between experiment and modeling in the Nernst-Planck approach: decontamination factor and normalized breakthrough curve (inset).